

N.V. Shevchenko

On a quasi-bound state in the K^-d system caused by strong interactions

Received: date / Accepted: date

Abstract It was found that NN potential could influence the results of the quasi-bound state search in the K^-d system, where the corresponding pole is situated close to the threshold. Three-body Faddeev-type calculations of the $\bar{K}NN - \pi\Sigma N$ system performed with a new model of nucleon-nucleon interaction predict the existence of the quasi-bound K^-d state caused by strong interactions. Its binding energy is small (1 – 2 MeV), while the width is comparable with the width of the K^-pp quasi-bound state (40 – 60 MeV).

Keywords Few-body exotic systems · AGS equations · Antikaon-nucleon interaction

1 Introduction

Many theoretical works and several experiments were devoted to the question of a quasi-bound state in systems consisting of an antikaon(s) and nucleons, see e.g. [1]. Particular interest was attracted to the lightest possible system $\bar{K}NN$ with zero spin (usually denoted as K^-pp): all theoretical works predicted the quasi-bound state in it. The methods of and the inputs for the calculations are quite different, and the predicted binding energy and width of the state also variate in quite a wide range. We also predicted a quasi-bound state in the spin zero $\bar{K}NN$ system [1] with binding energy and width strongly depending on the particular form of the antikaon-nucleon potential, which is used as a input. We solved three-body Faddeev-type AGS equations [2] with coupled $\bar{K}NN$ and $\pi\Sigma N$ channels and used three different models of $\bar{K}N$ interaction: two phenomenological potentials and one chirally motivated model.

We also studied another state of the $\bar{K}NN$ system with spin one (which will be denoted as K^-d). It has an atomic state, kaonic deuterium, which is mainly caused by Coulomb attraction between K^- and p , while the strong interactions give corrections to the binding energy and width (see [3] and references therein). But we did not find a pole caused by purely strong interactions corresponding to the quasi-bound state in K^-d [4] similar to that one in the K^-pp system. We demonstrated, that the strong quasi-bound state appears in the K^-d system if the attraction in the isospin-zero $\bar{K}N - \bar{K}N$ part of the coupled-channel $\bar{K}N - \pi\Sigma$ potential is increased by hands.

After studying $\bar{K}NN$ and $\bar{K}\bar{K}N$ systems (the last one also has a quasi-bound state [5]) we started investigations of the four-body $\bar{K}NNN$ system. We are using four-body Faddeev-type equations [6] on four-body transition amplitudes, which contain, among others, three-body transition amplitudes evaluated at every step of the four-body calculations. We constructed a new nucleon-nucleon potential

The work was supported by the Czech GACR grant 19-19640S.

N.V. Shevchenko
Nuclear Physics Institute, 25068 Řež, Czech Republic
E-mail: shevchenko@ujf.cas.cz

for these calculations, and found out that the quasi-bound state caused by the strong interactions appeared in the K^-d system. The present paper is devoted to this state.

2 Three-body AGS equations and two-body input

The calculations of the quasi-bound state in the K^-d system caused by strong interactions were performed using the same method and input as those used for the K^-pp system [1]. We solved Faddeev-type three-body equations in AGS form [2] with coupled $\bar{K}NN$ and $\pi\Sigma N$ channels. The three-body equations in operator form for the $\bar{K}NN$ system with spin one (K^-d) are those for the spin-one $\bar{K}NN$ (K^-pp): Eqs. (23–25) of [1]. Written in momentum representation they differ from the K^-pp case by the antisymmetrization and $6j$ recoupling coefficients.

The three-body AGS equations in momentum representation are integral equations. We solved them in two ways. One of them is the direct search of the pole position in the complex plane. Another one is the $1/|\text{Det}|^2$ method proposed and successively used for the K^-pp system in [7]. The idea of the method is that a pole, situated under the threshold, must be seen at the real energy axis as a bump. The position and the width of the quasi-bound state can be evaluated by fitting the bump by Breit-Wigner formula with some arbitrary background. The two methods supplement each other: the direct search needs initial values for the eigenvalue problem solving, and they can be provided by the $1/|\text{Det}|^2$ method. On the other hand, the binding energy and width obtained from bump fitting could be used as a control of the direct search result.

The input for the AGS equations describing the $\bar{K}NN - \pi\Sigma N$ system are T -matrices corresponding to the $\bar{K}N - \pi\Sigma$, NN , ΣN and πN potentials. All the potentials have separable form, which simplifies the three-body equations, all of them reproduce low-energy experimental data for the corresponding subsystem quite accurately. Keeping in mind uncertainties in experimental data used for construction of the interaction models, we see no reason to introduce some three-body force and by this increase ambiguity of the calculations. Coulomb interaction between K^- and p was not included into the equations, since in contrast to atomic state calculations, where Coulomb plays the main role, the present work is devoted to the quasi-bound K^-d state caused by strong interactions, where Coulomb should lead to some small corrections only.

Interaction of an antikaon with a nucleon plays the main role in the calculations. It is strongly attractive in the isospin zero state, which had lead to the question of a quasi-bound state in few- and/or many-body systems consisting of antikaon(s) and nucleons existence. The $\bar{K}N$ system is coupled to the $\pi\Sigma$ channel through the $\Lambda(1405)$ resonance, which is usually assumed as a resonance in the $\pi\Sigma$ channel and a quasi-bound state in the $\bar{K}N$ channel. The resonance is formed by one or two poles (this question rose quite vivid discussions) and, according to the Particle Data Group [8] has a mass $1405.1^{+1.3}_{-1.0}$ MeV and a width 50.5 ± 2.0 MeV.

We used three our models of antikaon-nucleon interaction, constructed and used before. They are: two phenomenological potentials with coupled $\bar{K}N$ and $\pi\Sigma$ channels and one- or two-pole structure of the $\Lambda(1405)$ resonance ($V_{\bar{K}N}^{1,\text{SIDD}}$ and $V_{\bar{K}N}^{2,\text{SIDD}}$ correspondingly), and the chirally motivated $\bar{K}N - \pi\Sigma - \pi\Lambda$ potential $V_{\bar{K}N}^{\text{Chiral}}$ (with two-pole $\Lambda(1405)$ structure). Parameters of the phenomenological and the chirally motivated potentials are presented in [23] and [4] correspondingly. Yamaguchi form-factors were used for the one-pole phenomenological and chirally motivated potentials together with the $\bar{K}N$ form-factor of the two-pole phenomenological potential. The $\pi\Sigma$ form-factor of the two-pole $V_{\bar{K}N}^{2,\text{SIDD}}$ has more complicated form. The chirally-motivated potential is energy-dependent one.

All three potentials were fitted to the experimental data on kaonic hydrogen and low-energy K^-p scattering. In particular, they reproduce $1s$ level shift and width in kaonic hydrogen, caused by the strong interaction additional to the main Coulomb interaction, measured by SIDDHARTA experiment [24]. In contrast to other authors we reproduce these observables directly without using a Deser-like approximate formula connecting the characteristics of kaon hydrogen with the K^-p scattering length. Our three models of the antikaon-nucleon interaction also reproduce elastic and inelastic cross-sections of K^-p scattering [9; 10; 11; 12; 13; 14] together with threshold branching ratios γ , R_c and R_n [15; 16] (or $R_{\pi\Sigma}$ constructed from the last two in the case of phenomenological potentials).

The phenomenological models with coupled $\bar{K}N$ and $\pi\Sigma$ channels were used in the three-body coupled-channel $\bar{K}NN - \pi\Sigma N$ calculations, while the corresponding exact optical $\bar{K}N(-\pi\Sigma)$ poten-

tials¹ were taken in approximate one-channel $\bar{K}N$ calculations. The chirally motivated $\bar{K}N - \pi\Sigma - \pi\Lambda$ interaction model was used as $\bar{K}N - \pi\Sigma(-\pi\Lambda)$ in the three-body calculation with coupled channels since three-body channel with Λ is not included into the equations. The exact optical $\bar{K}N(-\pi\Sigma - \pi\Lambda)$ version of interaction entered the approximate three-body equations.

Spin dependent and spin independent potentials of the ΣN interaction were constructed in [17]. They are one-term separable potentials with Yamaguchi form-factors. The parameters were fitted to the experimental data on ΣN and ΛN cross-sections [18; 19; 20; 21; 22]. Isospin 1/2 $\Sigma N - \Lambda N$ potential is a two-channel one, it is used in the three-body calculations in a form of the exact optical $\Sigma N(-\Lambda N)$ potential. The isospin 3/2 ΣN potential has only one channel. In the present calculations we used the ΣN interaction model, which does not depend on spin.

The πN potential is assumed to play negligible role, and was omitted. Finally, the new nucleon-nucleon potential, which lead to the K^-d quasi-bound state appearance, is described in the next section.

3 New separable NN potential

The Two-term Separable New potential (TSN) of nucleon-nucleon interaction has a form

$$V_{NN}^{\text{TSN}}(k, k') = \sum_{m=1}^2 g_m(k) \lambda_m g_m(k'), \quad (1)$$

with form-factors

$$g_m(k) = \sum_{n=1}^3 \frac{\gamma_{mn}}{(\beta_{mn})^2 + k^2}, \quad \text{for } m = 1, 2. \quad (2)$$

It was fitted to Argonne $V18$ potential [25] phase shifts without the condition, which was imposed on the previously used V_{NN}^{TSA} potential [26]: one of the normalization constants of the deuteron wave function must be equal to zero. Technically the new V_{NN}^{TSN} and previously used V_{NN}^{TSA} models differ by the number of terms in the form-factors, Eq.(2). The parameters of the new two-term separable potential are presented in Table 1 for the triplet and in Table 2 for the singlet case.

Table 1 Parameters of the new V_{NN}^{TSN} potential, triplet: strength constants λ_m , range β_{mn} and additional γ_{mn} parameters.

	λ_m	β_{m1}	β_{m2}	β_{m3}	γ_{m1}	γ_{m2}	γ_{m3}
$m = 1$	-1.9938	1.2096	3.2135	1.3912	0.0884	1.9889	-0.1027
$m = 2$	1.7584	3.9940	3.9999	2.7070	-1.9660	-1.9225	0.4144

Four parameters ($\lambda_m, \gamma_{m1}, \gamma_{m2}, \gamma_{m3}$) for every m can be replaced by three independent parameters ($\lambda'_m = \lambda_m * \gamma_{m3}^2, \gamma'_{m1} = \gamma_{m1}/\gamma_{m3}, \gamma'_{m2} = \gamma_{m2}/\gamma_{m3}$), correspondingly, with $\gamma'_{m3} = 1$. Therefore, np and pp potentials contain 12 independent parameters each. Such transformation does not change the potential Eq.(1) and can be done with γ_{m1} or γ_{m2} as well. However, the "natural" values of the parameters, presented in Tables 1 and 2 are more convenient for numerical calculations.

The triplet and singlet scattering lengths a and effective ranges r_{eff} provided by the TSN potential are:

$$a_{np}^{\text{TSN}} = -5.400 \text{ fm}, \quad r_{\text{eff}, np}^{\text{TSN}} = 1.744 \text{ fm} \quad (3)$$

$$a_{pp}^{\text{TSN}} = 16.325 \text{ fm}, \quad r_{\text{eff}, pp}^{\text{TSN}} = 2.792 \text{ fm}, \quad (4)$$

¹ The exact optical potential is the one-channel potential, which provides exactly the same elastic amplitude as the coupled-channel model of interaction (see e.g. [17]).

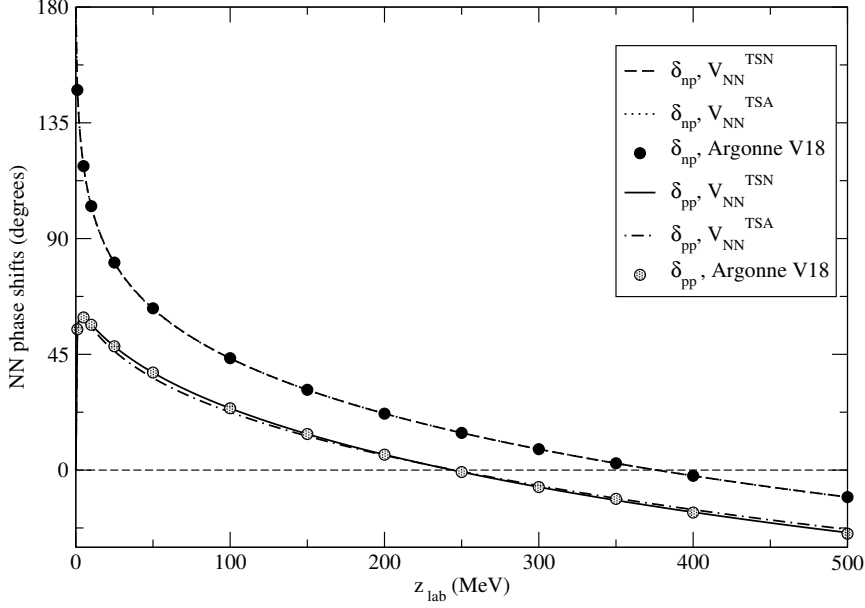


Fig. 1 Phase shifts of np and pp scattering calculated using the new V_{NN}^{TSN} and previously used $V_{NN}^{\text{TSA-B}}$ potentials (lines) compared with phase shifts of Argonne V18 potential (circles).

the binding energy of the deuteron is $E_{\text{deu}} = 2.2246$ MeV. The previously used TSA potential (its TSA-B version) provides slightly different scattering lengths and effective ranges:

$$a_{np}^{\text{TSA-B}} = -5.413 \text{ fm}, \quad r_{\text{eff}, np}^{\text{TSA-B}} = 1.760 \text{ fm} \quad (5)$$

$$a_{pp}^{\text{TSA-B}} = 16.559 \text{ fm}, \quad r_{\text{eff}, pp}^{\text{TSA-B}} = 2.880 \text{ fm} \quad (6)$$

and the same binding energy of deuteron (2.2246 MeV).

Table 2 Parameters of the new V_{NN}^{TSN} potential, singlet: strength constants λ_m , range $\beta_m n$ and additional γ_{mn} parameters.

	λ_m	β_{m1}	β_{m2}	β_{m3}	γ_{m1}	γ_{m2}	γ_{m3}
$m = 1$	-1.9793	1.8855	2.8396	1.1834	-0.1800	1.9999	0.0362
$m = 2$	1.7815	3.9897	3.9919	0.5000	-1.8881	-1.9914	0.0014

Phase shifts of np and pp scattering calculated using the new V_{NN}^{TSN} potential are plotted together with those calculated using TSA-B version of the previously used model in Figure 1. It is seen that the phase shifts given by Argonne V18 potential [25] (black circles for δ_{np} and circles filled with dots for δ_{pp}) are reproduced by the new potential with high accuracy. The phases of the new TSN and the previously used TSA-B potentials are practically indistinguishable for the case of δ_{np} (dashed and dotted lines), while pp phases are slightly different (solid and dash-dotted lines for TSN and TSA-B potentials correspondingly). The phases change their signs, which means that all three potentials are repulsive at short distances.

4 Results and discussion

The results of the direct search of the pole in the K^-d system corresponding to the quasi-bound state caused by strong interactions are shown in Table 3. The new nucleon-nucleon V_{NN}^{TSA} potential was used together with the three models of antikaon-nucleon interaction. The calculations with coupled $\bar{K}NN - \pi\Sigma N$ channels using the phenomenological $\bar{K}N$ potential with one-pole structure of the $\Lambda(1405)$ resonance $V_{\bar{K}N}^{1,\text{SIDD}}$ provide no quasi-bound state. In contrast to it, the models with two-pole structure: the phenomenological $V_{\bar{K}N}^{2,\text{SIDD}}$ and chirally-motivated $V_{\bar{K}N}^{\text{Chiral}}$ potentials, - provide a quasi-bound state with small binding energy B_{K^-d} . The energy is counted from the K^-d threshold $z_{th,K-d} = m_{\bar{K}} + 2m_N + E_{\text{deu}} = 2371.26$ MeV.

Table 3 Binding energy B_{K^-d} (MeV) and width Γ_{K^-d} (MeV) of the quasi-bound state in the K^-d system calculated using direct pole search in the complex energy plane. The results obtained by coupled-channel $\bar{K}NN - \pi\Sigma N$ equations solving and one-channel $\bar{K}NN$ variant with exact optical antikaon-nucleon potentials are presented. Phenomenological $\bar{K}N$ potentials with one-pole $V_{\bar{K}N}^{1,\text{SIDD}}$ and two-pole $\Lambda(1405)$ structure $V_{\bar{K}N}^{2,\text{SIDD}}$ were used together with the chirally-motivated model $V_{\bar{K}N}^{\text{Chiral}}$ of the antikaon-nucleon interaction. The binding energy is counted from the threshold energy of the K^-d system: $z_{th,K-d} = m_{\bar{K}} + 2m_N + E_{\text{deu}} = 2371.26$ MeV.

	Coupled-channels calculation		With exact optical $\bar{K}N$ potential	
	B_{K^-d}	Γ_{K^-d}	B_{K^-d}	Γ_{K^-d}
$V_{\bar{K}N}^{1,\text{SIDD}}$	—	—	0.8	68.3
$V_{\bar{K}N}^{2,\text{SIDD}}$	0.9	59.4	3.8	63.2
$V_{\bar{K}N}^{\text{Chiral}}$	1.3	41.8	0.9	43.6

No K^-d quasi-bound state was found in our previous work [4], where similar calculations were performed with V_{NN}^{TSA} potential. Therefore the particular model of nucleon-nucleon interaction, not only of antikaon-nucleon one, can influence the result of the quasi-bound pole search in the K^-d system.

It was demonstrated in [4] that gradual increasing of the absolute value of the isospin zero constant $\lambda_{I=0}^{\bar{K}K}$ of the $\bar{K}N - \pi\Sigma$ potential leads to the quasi-bound state appearance in the K^-d system. And the necessary changes are small, as minimum, for the system described by the two-pole phenomenological $\bar{K}N$ potential. Indeed, it is seen at Fig. 6 of [4], that the pole calculated with $V_{\bar{K}N}^{2,\text{SIDD}}$ potential with multiplication factor 1 is situated slightly above the K^-d threshold, so that the K^-d system is almost bound. On the other hand, we have shown in [17], that NN interaction plays a minor role in K^-d scattering length calculations. It is seen at Fig. 12 of [17] that use of PEST nucleon-nucleon potential which is not repulsive at short distances changes a_{K^-d} only slightly in comparison with the results obtained with V_{NN}^{TSA} (with is repulsive at short distances). Keeping all this in mind, the few MeV binding energy of the K^-d quasi-bound state caused by strong interactions is an expected result. The positions of the poles calculated with the previously used nucleon-nucleon V_{NN}^{TSA} potential are so close to the K^-d threshold (from above), that use of another V_{NN} pushes the poles downward under the threshold, so that the quasi-bound state appeared.

The widths of the K^-d quasi-bound states presented in Table 3 confirm our suggestions [4] that they must be comparable with those for the K^-pp quasi-bound state.

The results of the approximate calculations performed with the exact optical versions of the three antikaon-nucleon potentials are also shown in Table 3. In that case the quasi-bound state also appeared in the K^-d system described by the one-pole $V_{\bar{K}N}^{1,\text{SIDD}}$ potential in addition to the two others. The binding energies of the already existing K^-d quasi-bound states (described by the two-pole $V_{\bar{K}N}$) has changed, and they become broader.

An atomic state, kaonic deuterium (see [3] and references therein) exists in the spin one $\bar{K}NN$ system, however it cannot be misidentified with the quasi-bound state caused by the strong interactions.

Indeed, the binding energy of kaonic deuterium is ~ 10 keV, while strong interactions bound the system with $1 - 2$ MeV. The differences in widths of the atomic and strong K^-d states is even more drastic: tens of MeV for the strong quasi-bound states in contrast to ~ 1 keV for kaonic deuterium [3].

We also performed calculations of the $1/|\text{Det}|^2$ functions, which provided quite good results for the K^-pp system [7]. The bumps corresponding to the K^-pp poles evaluated with the three models of antikaon-nucleon interaction were clearly pronounced and have a resonance-like form. On the contrary, the K^-d bumps in the $1/|\text{Det}|^2$ functions are situated very close to the $\bar{K}NN$ threshold and are not clearly pronounced, especially those obtained with the phenomenological potentials. It is seen in Figure 2, where the points calculated using one-pole phenomenological $V_{\bar{K}N}^{1,\text{SIDD}}$ (circles), two-pole phenomenological $V_{\bar{K}N}^{2,\text{SIDD}}$ (triangles) and chirally motivated $V_{\bar{K}N}^{\text{Chiral}}$ (squares) potentials are joined by the fitting lines. Breit-Wigner fits of the calculated $1/|\text{Det}|^2$ functions with arbitrary background in the K^-d system are far not so accurate as in the case of K^-pp system:

$$\begin{aligned} B_{K^-d,BW}^{1,\text{SIDD}} &= 9.2 \text{ MeV}, & \Gamma_{K^-d,BW}^{1,\text{SIDD}} &= 59.6 \text{ MeV}, \\ B_{K^-d,BW}^{2,\text{SIDD}} &= 11.4 \text{ MeV}, & \Gamma_{K^-d,BW}^{2,\text{SIDD}} &= 52.2 \text{ MeV}, \\ B_{K^-d,BW}^{\text{Chiral}} &= 5.3 \text{ MeV}, & \Gamma_{K^-d,BW}^{\text{Chiral}} &= 48.6 \text{ MeV}. \end{aligned} \quad (7)$$

It seems that the $1/|\text{Det}|^2$ method is not good for quasi-bound states situated so close to the threshold.

For comparison we studied, how the new NN potential changes binding energies and widths of the K^-pp quasi-bound states. The results are presented in Table 4, where the characteristics of the K^-pp quasi-bound state calculated using the system of equations with coupled $\bar{K}NN$ and $\pi\Sigma N$ channels are shown together with the results of one-channel calculations with exact optical $\bar{K}N$ potentials. The K^-pp binding energies and widths obtained with the previously use TSA-B NN potential and published in [7] are also shown. The binding energy is counted from the threshold energy of the K^-pp system: $z_{th,K^-pp} = m_{\bar{K}} + 2m_N = 2373.485$ MeV. It is seen that the new model of NN interaction also

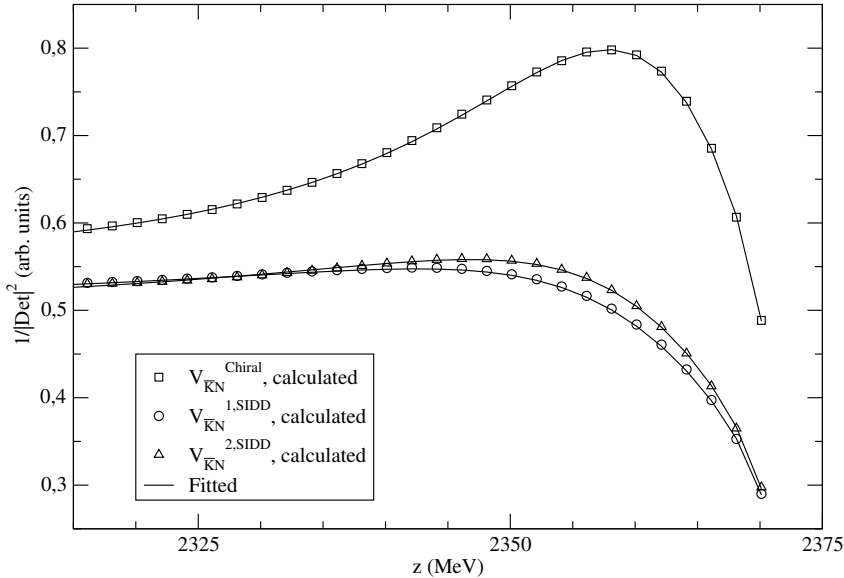


Fig. 2 Evaluated $1/|\text{Det}(z)|^2$ functions for the K^-d system calculated using chirally-motivated $V_{\bar{K}N}^{\text{Chiral}}$ (squares), one-pole phenomenological $V_{\bar{K}N}^{1,\text{SIDD}}$ (circles) and two-pole phenomenological $V_{\bar{K}N}^{2,\text{SIDD}}$ (triangles) antikaon-nucleon potentials. The lines are the corresponding non-linear fits of the functions.

changed the pole positions on few MeV. However, since the quasi-bound state in the K^-pp system, in contrast to K^-d , is situated far from the $\bar{K}NN$ and $\pi\Sigma N$ thresholds, these changes do not have so drastic effect.

Table 4 Binding energy B_{K^-pp} (MeV) and width Γ_{K^-pp} (MeV) of the quasi-bound state in the K^-pp system calculated using direct pole search in the complex energy plane. The results obtained by coupled-channel $\bar{K}NN - \pi\Sigma N$ equations solving and one-channel $\bar{K}NN$ variant with exact optical antikaon-nucleon potentials are presented. Phenomenological $\bar{K}N$ potentials with one-pole $V_{\bar{K}N}^{1,\text{SIDD}}$ and two-pole $\Lambda(1405)$ structure $V_{\bar{K}N}^{2,\text{SIDD}}$ were used together with the chirally-motivated model $V_{\bar{K}N}^{\text{Chiral}}$ of the antikaon-nucleon interaction. Previous results from [7] are also shown. The binding energy is counted from the threshold energy of the K^-pp system: $z_{th,K^-pp} = m_{\bar{K}} + 2m_N = 2373.485$ MeV.

	Coupled channels calculation		With exact optical $\bar{K}N$ potential		Previous results from [7]	
	B_{K^-pp}	Γ_{K^-pp}	B_{K^-pp}	Γ_{K^-pp}	B_{K^-pp}	Γ_{K^-pp}
$V_{\bar{K}N}^{1,\text{SIDD}}$	52.18	67.1	53.29	63.3	53.29	64.9
$V_{\bar{K}N}^{2,\text{SIDD}}$	46.56	51.2	46.65	47.4	47.45	49.8
$V_{\bar{K}N}^{\text{Chiral}}$	29.43	46.4	30.01	46.6	32.24	48.6

Comparing the K^-d and K^-pp characteristics of the quasi-bound states caused purely by strong interactions in Tables 3 and 4 correspondingly, we see large difference between the binding energies in the both systems: the K^-pp is bound much stronger than K^-d . The K^-d and K^-pp widths are comparable. We see, that the particular model of V_{NN} plays a minor role in the K^-pp system, differences in the pole positions (below and above the threshold) in the K^-d system are also not very big. However, since the K^-d poles are situated very close to the K^-d threshold, these small differences resolve the question of the quasi-bound state existence.

5 Summary

We found that NN potential could influence the results of the quasi-bound state search in the K^-d system, where the corresponding pole is situated close to the K^-d threshold, and predicted possibility of the K^-d quasi-bound state existence caused by the strong interactions. Three-body Faddeev-type calculations performed with the new TSN model of nucleon-nucleon interaction found out the quasi-bound state in this system with binding energy 1 – 2 MeV and width comparable with those obtained for the K^-pp system, 40 – 60 MeV. The quasi-bound state caused by strong interactions is stronger bound and is much broader than kaonic deuterium, therefore, the atomic and the strong quasi-bound states cannot be misidentified.

References

1. N.V. Shevchenko, N.V.: Three-Body AntikaonNucleon Systems. *Few Body Syst.* 58, 6 (2017)
2. Alt, E.O., Grassberger, P., Sandhas, W.: Reduction of the three-particle collision problem to multi-channel two-particle Lippmann-Schwinger equations. *Nucl. Phys. B* 2, 167 (1967)
3. Révai, J.: Three-body calculation of the $1s$ level shift in kaonic deuterium with realistic $\bar{K}N$ potentials. *Phys. Rev. C* 94, 054001 (2016)
4. Shevchenko, N.V., Révai, J.: Faddeev calculations of the $\bar{K}NN$ system with chirally-motivated $\bar{K}N$ interaction. I. Low-energy K^-d scattering and antikaonic deuterium. *Phys. Rev. C* 90, 034003 (2014)
5. Shevchenko, N.V., Haidenbauer, J.: Exact calculations of a quasibound state in the $\bar{K}KN$ system. *Phys. Rev. C* 92, 044001 (2015)
6. Grassberger, P., Sandhas, W.: Systematical treatment of the non-relativistic n-particle scattering problem. *Nucl. Phys. B* 2, 181 (1967)

-
7. Révai, J., Shevchenko, N.V.: Faddeev calculations of the $\bar{K}NN$ system with chirally-motivated $\bar{K}N$ interaction. II. The K^-pp quasi-bound state. Phys. Rev. C 90, 034004 (2014)
 8. Olive K.A. et al. (Particle Data Group): The Review of Particle Physics (2015). Chin. Phys. C, 38, 090001 (2014) and 2015 update
 9. Sakitt, M. et al.: Low-energy K^- -meson interactions in hydrogen. Phys. Rev. 139, B 719 (1965)
 10. Kim, J.K.: Low-energy K^-p interaction and interpretation of the 1405-MeV Y_0^* resonance as a $\bar{K}N$ bound state. Phys. Rev. Lett. 14, 29 (1965)
 11. Kim, J.K.: Multichannel phase-shift analysis of $\bar{K}N$ interaction in the region 0 to 550 MeV/c. Phys. Rev. Lett. 19, 1074 (1967)
 12. Kittel, W., Otter, G., Wacek, I.: The K^- proton charge exchange interactions at low energies and scattering lengths determination. Phys. Lett. 21, 349 (1966)
 13. Ciborowski, J. et al.: Kaon scattering and charged Sigma hyperon production in K^-p interactions below 300 MeV/c. J. Phys. G 8, 13 (1982)
 14. Evans, D. et al.: Charge-exchange scattering in K^-p interactions below 300 MeV/c. J. Phys. G 9, 885 (1983)
 15. Tovee, D.N. et al.: Some properties of the charged Σ hyperons. Nucl. Phys. B 33, 493 (1971)
 16. Nowak, R.J. et al.: Charged Σ hyperon production by K^- meson interactions at rest. Nucl. Phys. B 139, 61 (1978)
 17. Shevchenko, N.V.: One- versus two-pole $\bar{K}N - \pi\Sigma$ potential: K^-d scattering length. Phys. Rev. C 85, 034001 (2012)
 18. Alexander, G. et al.: Study of the $\Lambda - N$ system in low-energy $\Lambda - p$ elastic scattering. Phys. Rev. 173, 1452 (1968)
 19. Sechi-Zorn, B., Kehoe, B., Twitty, J., Burnstein, R.A.: Low-energy Λ -proton elastic scattering. Phys. Rev. 175, 1735 (1968)
 20. Eisele, F. et al.: Elastic $\Sigma^\pm p$ scattering at low energies. Phys. Lett. B 37, 204 (1971)
 21. Engelmann, R., Filthuth, H., Hepp, V., Kluge, E.: Inelastic $\Sigma^- p$ -interactions at low momenta. Phys. Lett. 21, 587 (1966)
 22. Hepp, V., Schleich, M.: A new determination of the capture ratio $r_c = \frac{\Sigma^- p \rightarrow \Sigma^0 n}{(\Sigma^- p \rightarrow \Sigma^0 n) + (\Sigma^- p \rightarrow \Lambda^0 n)}$, the Λ^0 -lifetime and the $\Sigma^- - \Lambda^0$ mass difference. Z. Phys. 214, 71 (1968)
 23. Shevchenko, N.V.: Near-threshold K^-d scattering and properties of kaonic deuterium. Nucl. Phys. A 890-891, 50-61 (2012)
 24. Bazzi, M. *et al.* (SIDDHARTA Collaboration): A new measurement of kaonic hydrogen X-rays. Phys. Lett. B 704, 113 (2011)
 25. Wiringa, R.B., Stoks, V.G.J., Schiavilla, R.: Accurate nucleon-nucleon potential with charge-independence breaking. Phys. Rev. C 51, 38 (1995)
 26. Doleschall, P.: *private communication*